

Light Induces Ultrastructural Changes in Rod Outer and Inner Segments, Including Autophagy, in a Transgenic *Xenopus laevis* P23H Rhodopsin Model of Retinitis Pigmentosa

Tami H. Bogéa, Runxia H. Wen, and Orson L. Moritz

Department of Ophthalmology and Visual Sciences and Centre of Macular Research, University of British Columbia, Vancouver, British Columbia, Canada

Correspondence: Orson L. Moritz, Department of Ophthalmology & Visual Sciences, University of British Columbia, 2550 Willow Street, Vancouver, BC, Canada V5Z 3N9; olmoritz@mail.ubc.ca.

Submitted: March 4, 2015
Accepted: November 5, 2015

Citation: Bogéa TH, Wen RH, Moritz OL. Light induces ultrastructural changes in rod outer and inner segments, including autophagy, in a transgenic *Xenopus laevis* P23H rhodopsin model of retinitis pigmentosa. *Invest Ophthalmol Vis Sci*. 2015;56:7947–7955. DOI:10.1167/iov.15-16799

PURPOSE. We previously reported a transgenic *Xenopus laevis* model of retinitis pigmentosa in which tadpoles express the bovine form of P23H rhodopsin (bP23H) in rod photoreceptors. In this model, retinal degeneration was dependent on light exposure. Here, we investigated ultrastructural changes that occurred in the rod photoreceptors of these retinas when exposed to light.

METHODS. Tadpoles expressing bP23H in rods were transferred from constant darkness to a 12-hour light:12-hour dark (12L:12D) regimen. For comparison, transgenic tadpoles expressing an inducible form of caspase 9 (iCasp9) were reared in a 12L:12D regimen, and retinal degeneration was induced by administration of the drug AP20187. Tadpoles were euthanized at various time points, and eyes were processed for confocal light and transmission electron microscopy.

RESULTS. We observed defects in outer and inner segments of rods expressing bP23H that were aggravated by light exposure. Rod outer segments exhibited vesiculations throughout and were rapidly phagocytosed by the retinal pigment epithelium. In rod inner segments, we observed autophagic compartments adjacent to the endoplasmic reticulum and extensive vesiculation at later time points. These defects were not found in rods expressing iCasp9, which completely degenerated within 36 hours after drug administration.

CONCLUSIONS. Our results indicate that ultrastructural defects in outer and inner segment membranes of bP23H expressing rods differ from those observed in drug-induced apoptosis. We suggest that light-induced retinal degeneration caused by P23H rhodopsin occurs via cell death with autophagy, which may represent an attempt to eliminate the mutant rhodopsin and/or damaged cellular compartments from the secretory pathway.

Keywords: autophagy, cell death, P23H, photoreceptor, retinitis pigmentosa, rhodopsin

Retinitis pigmentosa (RP) is a heterogeneous group of inherited diseases that results in progressive loss of vision in humans.¹ Over 100 mutations in the rhodopsin gene have been found to cause RP. The most common mutation found in North American patients is a single-base substitution at codon 23 (P23H).² P23H rhodopsin has been classified as a class II mutant because it misfolds, is retained in the endoplasmic reticulum (ER), and is not readily reconstituted by 11-*cis*-retinal.³

We previously investigated photoreceptor death in a P23H rhodopsin light-induced model of retinal degeneration.^{4–7} In *Xenopus laevis* tadpoles expressing the bovine form of P23H rhodopsin (bP23H), the photoreceptors degenerate rapidly when exposed to cyclic light. When reared in the dark, however, they are rescued from degeneration.^{4–6}

Degenerating photoreceptors expressing P23H rhodopsin exhibit ultrastructural defects in rod outer segments. Sakami et al.⁸ described the presence of disks parallel to the axoneme in rods of transgenic mice expressing this mutation, and vesiculotubular structures of 50 to 400 nm in diameter

occurred in rod outer segments of transgenic *X. laevis* expressing a rhodopsin-P23H-GFP fusion protein.⁹

The exact mechanisms of cellular toxicity caused by P23H rhodopsin remain unclear. Our previous studies suggest a mechanism involving the destabilization of P23H rhodopsin on loss of chromophore binding during light exposure, leading to decreased ER exit of the mutant rhodopsin,^{5,7} which likely causes photoreceptor death via activation of ER stress pathways.^{10–12} Alternatively, destabilization of the mutant rhodopsin located in photoreceptor outer segment membranes⁹ as well as oxidative stress¹³ could contribute to the cell death mechanism.

Previous studies suggest that autophagy, a process by which cells regulate the synthesis, degradation, and recycling of their products by using the lysosomal machinery,¹⁴ may also play a role in the process of photoreceptor degeneration. In several mouse models (rd, rds, and light-damaged albino mouse models), type II cell death, also known as cell death with autophagy,¹⁵ was implicated in the clearing of protein

aggregates and in the removal of cellular compartments in mutant or damaged retinas.¹⁶⁻¹⁹

In the present study, we report light-induced ultrastructural defects in both rod outer segment and rod inner segment membranes in a transgenic *X. laevis* bP23H rhodopsin model of RP. Using transmission electron microscopy (TEM), immunohistochemistry, and confocal microscopy, we also detected evidence of cell death with autophagy in inner segment membranes of rods expressing this mutation.

METHODS

Generation and Maintenance of Transgenic

X. laevis Tadpoles

All procedures adhered to the Association for Research in Vision and Ophthalmology statement for the use of animals in ophthalmic and visual research. Transgenic *X. laevis* tadpoles expressing bP23H in rods were generated by mating heterozygous male frogs carrying this transgene under the control of the *X. laevis* opsin promoter with wild-type female frogs.⁴ Tadpoles were then transferred to an 18°C incubator with a 24-hour day (constant dark) regimen. At day 14 post fertilization, they were transferred to a 12-hour light:12-hour dark (12L:12D; cyclic light) regimen (light intensity of 1700 lux) and were euthanized at various time points. Wild-type sibling tadpoles raised under the same conditions were used as negative controls.

Transgenic *X. laevis* tadpoles expressing eGFP and iCasp9 in rods were generated by mating heterozygous male frogs carrying the transgenes under the control of the *X. laevis* opsin promoter with wild-type female frogs.^{20,21} Tadpoles were then transferred to an 18°C incubator with a 12L:12D regimen (light intensity of 1700 lux). At day 14 post fertilization, rod photoreceptor death was induced by the addition of 10 nM of the compound AP20187 (Ariad Pharmaceuticals, Cambridge, MA, USA) to the tadpole medium, as described elsewhere.^{20,21} The tadpoles were euthanized at various time points. All animal procedures were performed in accordance with the ARVO Statement for the Use of Animals in Ophthalmic and Vision Research.

Dot Blot Genotyping

Eyes were processed for dot blots and imaged as Western blots according to procedures described in Tam et al.²² using the anti-rhodopsin mouse monoclonal antibodies B630N (gift from W. Clay Smith)²³ and 1D4 (EMD Millipore, Darmstadt, Germany).²⁴

Transmission Electron Microscopy

Eyes were fixed in a cold solution of 1% glutaraldehyde and 4% paraformaldehyde in 0.1 M sodium cacodylate buffer (pH 7.4), rinsed in 0.1 M sodium cacodylate buffer overnight, postfixed in a cold solution of 1% osmium tetroxide in 0.1 M sodium cacodylate buffer, and rinsed in buffer. They were dehydrated in a graded series of ethanol, ethanol/propylene oxide mixtures, and 100% propylene oxide, and finally embedded in Eponate-12 resin (Ted Pella, Redding, CA, USA). Gold serial sections from at least three eyes were cut for each time point, using an MT-5000 Sorvall microtome with a diamond knife (ThermoScientific, Waltham, MA, USA), mounted on coated copper grids, stained with 2% uranyl acetate and Venable and Coggleshall's lead citrate,²⁵ and examined using TEM (80 kV; model H7600; Hitachi, Tokyo, Japan).

Immunohistochemistry

Eyes were fixed overnight in a solution of 4% paraformaldehyde in 0.1 M phosphate buffer (pH 7.4), infiltrated in a solution of 20% sucrose in 0.1 M phosphate buffer for up to 2 hours, embedded in optimal cutting temperature (OCT) compound, and cryosectioned according to standard procedures.²²

Frozen serial sections (12 µm thick) were labeled with anti-light chain 3 (LC3)A/B rabbit polyclonal antibody (product code Ab128025; AbCam, Cambridge, UK) at 1:1000 dilution or anti-arrestin polyclonal antibody²⁶ (a gift from W. Clay Smith) at 1:1000 dilution, followed by anti-rabbit Cy3 conjugated secondary antibody (Jackson ImmunoResearch, West Grove, PA, USA) at 1:750 dilution. Sections were counterstained with wheat germ agglutinin (WGA) conjugated to Alexa 488 (Molecular Probes/Invitrogen, Grand Island, NY, USA) at 1:100 dilution and Hoechst 33342 nuclear stain at 1:1000 dilution (Sigma-Aldrich Corp., St. Louis, MO, USA). Labeled sections obtained from ten eyes of each experimental group were imaged using a Zeiss model 510 meta laser scanning confocal microscope (using a 1.2 numerical aperture 40× water immersion lens; Carl Zeiss, Munich, Germany). For LC3 quantification, labeled sections ($n \geq 4$ per group) were imaged at consistent depth (3 µm) and microscope settings. LC3 puncta were counted within three to five well-defined rod inner segments per image (chosen based on the WGA channel without reference to the LC3 channel).

RESULTS

X. laevis Tadpoles Expressing bP23H in Rods Exhibited Light-Induced Retinal Degeneration

We investigated the morphology of wild-type and transgenic photoreceptors of *X. laevis* kept under cyclic light conditions by using laser scanning confocal microscopy. For this purpose, tadpoles were reared without light exposure until 14 days post fertilization (dpf). They were then transferred to cyclic light, euthanized after 48 hours, processed for dot blot analysis (data not shown) and immunohistochemistry, and imaged by laser scanning confocal microscopy. Detection of bP23H rhodopsin in solubilized retinas using dot blots allowed retroactive discrimination of wild-type and transgenic tadpoles, as previously described.⁴

We observed severe retinal degeneration in the transgenic tadpole retinas after 48 hours of cyclic light exposure. Retinas expressing bP23H exhibited rod loss and abnormal morphology relative to retinas of wild-type animals reared in the dark or cyclic light, or retinas of transgenic animals reared in the dark (Figs. 1A-D). In particular, we noted the presence of shortened and absent rod outer segments (ROS) relative to those in wild-type animals or dark-reared transgenic animals.

Light Exposure Induced Defects in Rod Outer and Inner Segments of bP23H-Expressing Retinas

We investigated the internal ultrastructure of bP23H-expressing photoreceptors in tadpoles kept in darkness or cyclic light. Transgenic and wild-type tadpoles were reared in darkness until 14 dpf, then transferred to cyclic light, euthanized at various time points, and processed for TEM. At least three samples were examined for each condition.

We detected ultrastructural defects in rod outer and inner segment membranes of bP23H-expressing retinas (Fig. 2). Throughout the rod outer segments of dark-reared transgenic tadpoles, we observed alterations in ROS disk structure (Figs.

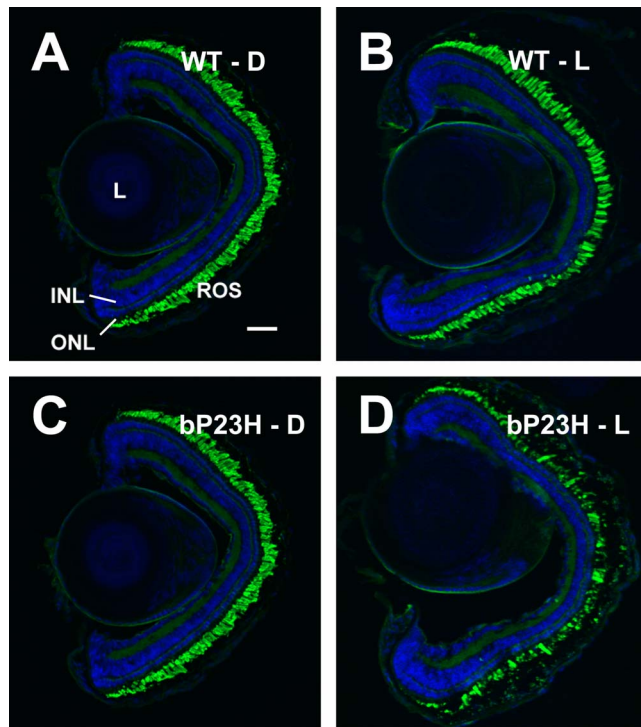


FIGURE 1. *Xenopus laevis* expressing bP23H rhodopsin in rods exhibited retinal degeneration when kept in cyclic light. (A) Wild-type tadpole kept in darkness (WT-D). (B) Wild-type tadpole kept in two light cycles (WT-L). (C) bP23H-expressing tadpole kept in darkness (bP23H-D). (D) bP23H-expressing tadpole kept in two light cycles totaling 24 hours of light (12L:12D:12L:12D) (bP23H-L). INL, inner nuclear layer; L, lens; ONL, outer nuclear layer. Scale bar: 100 μ m.

2C, 2D). Defects were arranged parallel to the plane of the disks, suggesting that some disks were dramatically affected throughout their diameter, whereas others were relatively unaffected. Defects included altered spacing between disks and vesiculations. These defects were exacerbated by light exposure (Figs. 2E, 2F, 2G, 2H), which increased the proportion of disk membranes affected. The membrane distortions became more severe, some disks adopted altered orientations (Fig. 2F), and the perimeter of the outer segment became very irregular. This was observed as early as 2 hours after the tadpoles were transferred to cyclic light (Figs. 2E, 2F). Neither vesiculations nor altered disks were observed in cone outer segments (Fig. 2G) nor in photoreceptors of wild-type tadpoles reared in the dark (Fig. 2A) or cyclic light (Fig. 2B). Rare unaffected rods (Fig. 2G) likely represent nonexpressing cells due to transgene silencing.²⁷

We also observed defects in rod inner segments (RIS) of bP23H-expressing retinas. Specifically, compartments consistent with the autophagy process occurred in the vicinity of the ER in dark-reared tadpoles (Fig. 3A). The number of these compartments was increased by light exposure (Figs. 3B, 3C, 3E) in transgenic tadpoles but was low in wild-type tadpoles kept either in constant darkness (not shown) or exposed to light (Fig. 3D). Dilation of ER cisternae was also observed (Figs. 3A-C). At later time points (Fig. 3C) massive vacuolization occurred.

The internal ultrastructure of these compartments was studied with TEM at higher magnifications (Fig. 4). Vesicle contents were often similar to those of the surrounding photoreceptor cell cytoplasm and included ribosomes and endoplasmic reticulum membranes (Figs. 4A, 4C, 4D),

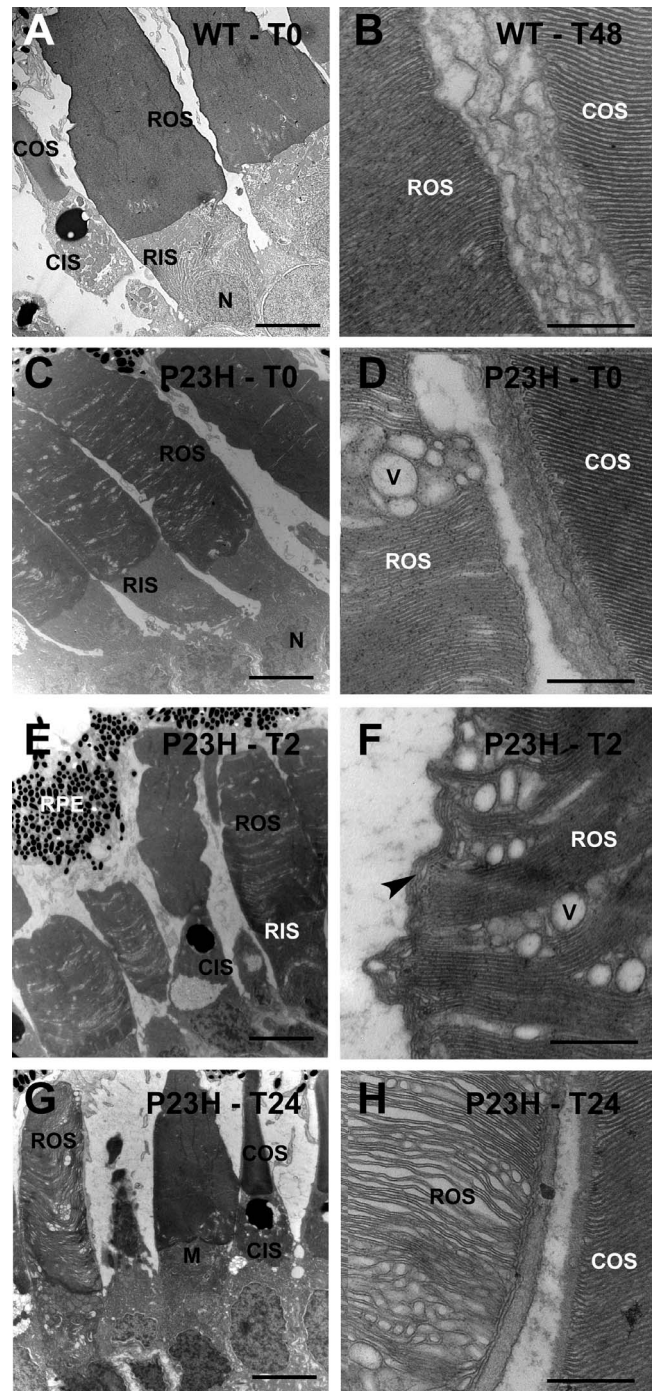


FIGURE 2. Light exposure exacerbated defects in rod outer segments of bP23H-expressing tadpoles. (A) Dark-reared WT tadpole. (B) Cyclic-light-reared WT tadpole. (C, D) Dark-reared bP23H-expressing tadpole. (E, F) bP23H-expressing tadpole exposed to 2 hours of light. (G, H) bP23H-expressing tadpole exposed to one complete light cycle consisting of 12L:12D. Note presence of ROS vesiculations and disks with abnormal orientations (*arrowhead*). COS, cone outer segment; CIS, cone inner segment; M, mitochondria; N, nucleus; V, vesiculation. Scale bars: 10 μ m (A, C, E, G), 500 nm (B, D, F, H).

suggesting autophagosomes or autolysosomes, whereas other compartments exhibited electron-dense contents or were relatively featureless (Figs. 4B, 4F), possibly representing more advanced stages with degraded contents, an entirely different vesicle population, or a combination of these two

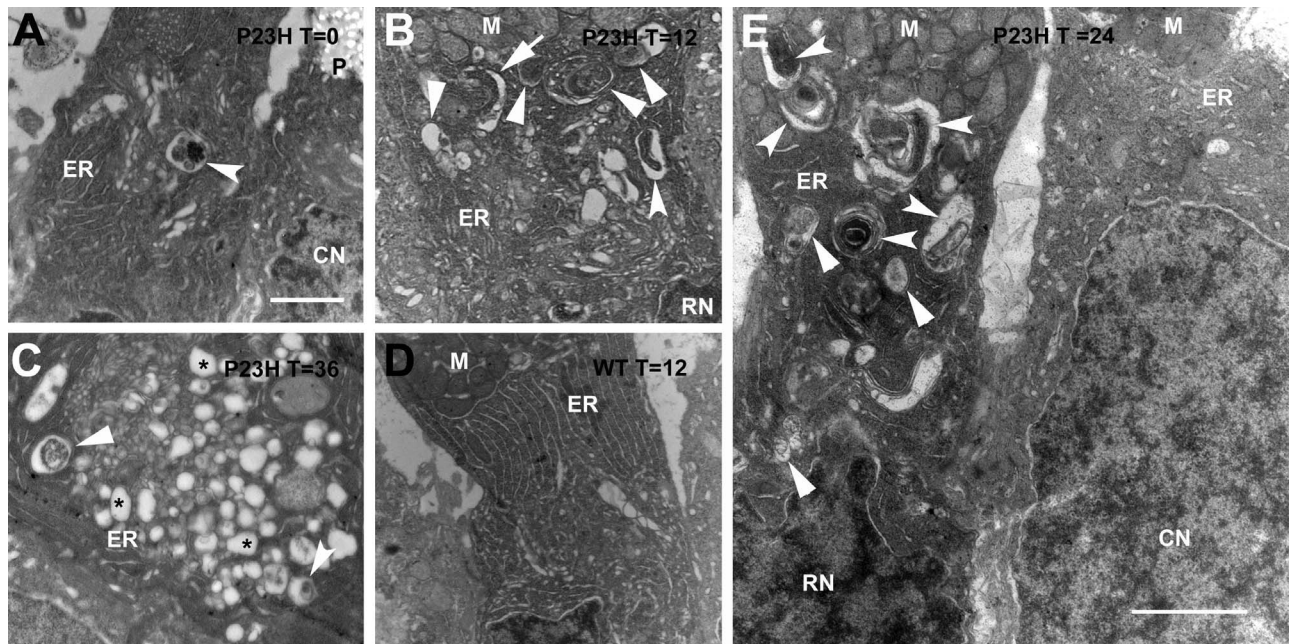


FIGURE 3. Light exposure exacerbated defects in rod inner segments of bP23H-expressing tadpoles. Note the presence of compartments with prominent contents (*arrowheads*), consistent with autophagosomes (*arrowheads*) or autolysosomes (*beveled arrowheads*). Possible phagophore formation (*arrow*) and numerous vesicular structures without identifiable contents (*asterisks*) are also present. (A) Dark-reared bP23H-expressing tadpole. (B) Dark-reared bP23H-expressing tadpole exposed to 12 hours of light. (C) bP23H-expressing tadpole kept in 1.5 light cycles (12L:12D:12L). (D) Wild-type tadpole reared in constant darkness and exposed to 12 hours of light. (E) Juxtaposed rod (*left*) and cone (*right*) inner segments from a transgenic tadpole kept in one complete light cycle. CN, cone nucleus; P, cone paraboloid. Scale bars: 2 μ m.

possibilities. Occasional examples consistent with mitophagy (autophagy of mitochondria) were observed (Fig. 4C). A double-membrane structure was often observed in vesicles with discernable contents (Figs. 4B, 4D, 4E), consistent with autophagosomes.²⁸

Outer Segment Defects Are Accompanied by Defective Trafficking of Arrestin

We reasoned that the outer segment defects we observed by TEM might interfere with the normal movement of soluble proteins between disks and between outer and inner segments. The protein arrestin, which is responsible for shutting off the signaling by photoactivated rhodopsin, is found primarily in the inner segments of dark-adapted *X. laevis* photoreceptors but migrates to the outer segment after short light exposures and returns to the inner segment after prolonged exposures.^{26,29} We examined the trafficking of this molecule in *X. laevis* photoreceptors expressing bP23H rhodopsin. Arrestin was found almost exclusively in the inner segment and axoneme in dark reared retinas of either genotype (Figs. 5A, 5B). However, rods expressing bP23H rhodopsin showed significant outer segment (OS) labeling with arrestin after a 12-hour light exposure (Fig. 5D), whereas wild-type retinas did not (Fig. 5C), indicating that the return of arrestin to the rod inner segment after prolonged light exposure was impaired.

Double-Membrane Compartments Found in Rod Inner Segments of bP23H Expressing Retinas Were Autophagic Compartments

To verify the presence of autophagosomes in these cells by an alternate method, tadpole eyes were labeled with a polyclonal

antibody raised against the microtubule-associated protein 1B-LC3,³⁰ which specifically associates with autophagosomes and autolysosomes.³¹ The antibody recognizes both LC3I (soluble) and LC3II (cleaved, lipidated, and associated with autophagosomes) forms. Punctate LC3 labeling confirmed the presence of autophagic compartments in wild-type and bP23H-expressing retinas of tadpoles kept in the dark or exposed to light for 12 hours. Figures 6A through 6E show that these compartments were located in rod inner segments, but they were also observed in all other retinal cell layers, and in the outer segment layer. Relative to WT siblings, we observed increased numbers of puncta in light-exposed bP23H photoreceptors (Fig. 6F), confirming results obtained by electron microscopy. Light chain 3-positive puncta located in the OS layer were likely associated with interdigitating processes of the retinal pigment epithelium (Figs. 6G-I), and therefore were not included in counts shown in Figure 6F.

Ultrastructural Changes Associated With Cell Death in a Drug-Induced Rod Apoptosis Model Differed From Those Induced by Light in the bP23H Model

The internal ultrastructure of iCasp9-expressing retinas was also studied as an experimental control in which cell death is not light-dependent, and occurs via activation of the apoptotic cascade. For this purpose, wild-type and transgenic tadpoles were reared in cyclic light. At 14 dpf, we administered AP20187 to induce rod photoreceptor death. The tadpoles were euthanized at various time points and processed for TEM.

By 48 hours, rod death was complete, and all rod remnants had been phagocytosed by the RPE (Fig. 7H). Prior to loss of rod photoreceptor integrity, the most notable feature was electron dense cytoplasm relative to other retinal cell types

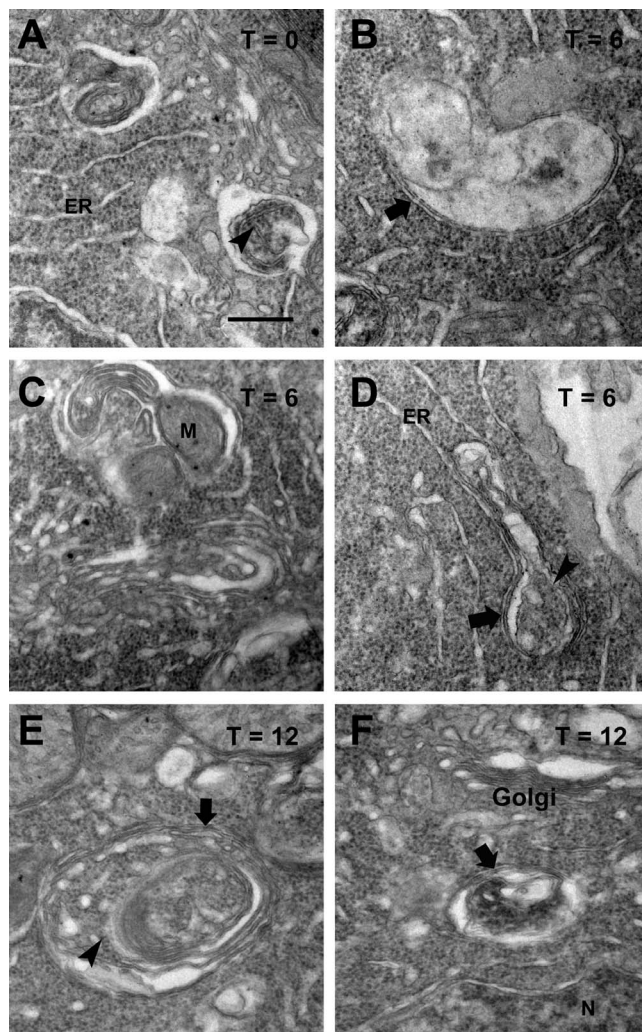


FIGURE 4. Double-membrane compartments are ultrastructurally consistent with autophagic compartments. Note the presence of double-membrane lining (*arrows*) and of ribosomes and endoplasmic reticulum membranes within the compartments (*arrowheads*). Images are from rod inner segments of dark-reared bP23H-expressing tadpole (A); bP23H-expressing tadpole exposed to light for 6 hours (B–D). (C) An example consistent with mitophagy. (E, F) bP23H-expressing tadpole exposed to 12 hours of light. *Scale bar:* 500 nm.

(Figs. 7B, 7C). Ultrastructural features present in degenerating bP23H rods were absent in degenerating iCasp9 rods (Figs. 7A–F). In rod outer segments, disks were stacked in an orderly fashion, and no vesiculations were seen in outer segments at any time point (Figs. 7C, 7D). Even fragments of rod OS present in RPE phagosomes at late time points retained a high degree of disk organization (Fig. 7F). We did not observe extensive vesiculation, structures consistent with autophagosomes, or similar membrane abnormalities of rod inner segments during the course of photoreceptor cell death.

DISCUSSION

Our results indicate that unique alterations in membrane ultrastructure were present in rod photoreceptors expressing bP23H rhodopsin, including defects in both outer and inner segment membranes. These defects were not present in WT rods or in rods degenerating due to other cell death

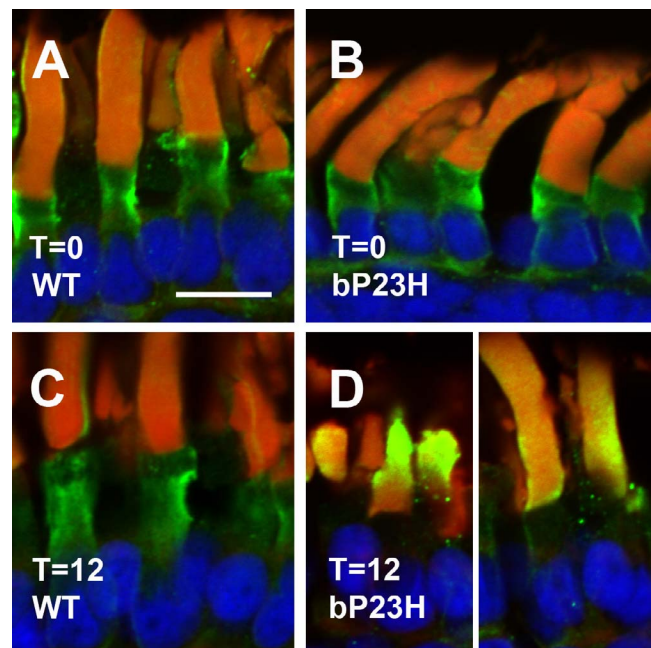


FIGURE 5. Arrestin localization is abnormal in light-exposed bP23H retinas. (A) Dark-reared, WT. (B) Dark-reared, bP23H. (C) WT, 12 hours of light exposure. (D) bP23H, 12 hours of light exposure. Arrestin immunolabeling is shown in *green*, wheat germ agglutinin in *red*, and Hoechst 33342 in *blue*. Distribution of arrestin is altered in light-exposed bP23H photoreceptors, with increased outer segment labeling. *Scale bar:* 10 μ m.

mechanisms. Furthermore, light exposure exacerbated these ultrastructural defects.

In rod outer segments, we observed vesiculations and altered disks in dark-reared animals that increased on light exposure. These vesiculations resembled the vesiculotubular structures previously described in transgenic *X. laevis* expressing the P23H rhodopsin-GFP fusion protein.⁹ We also observed the presence of altered disk orientations as reported by Sakami et al.⁸ in P23H knock-in mice. Outer segment disk membranes were sufficiently disrupted that the normal trafficking of arrestin between outer and inner segments was impaired. It is likely that the rapid light-induced alterations we observed occurring throughout the outer segments are the result of light-induced destabilization of P23H rod opsin in disks altering membrane protein packing density and inducing membrane conformational changes.

However, our results are also unique in that we observed significant ultrastructural alterations in inner segments, although previous studies also support the hypothesis that a biosynthetic defect leads to ER stress and cell death, and vacuolization was observed in a subset of rods in homozygous P23H knock-in mice.³² Moreover, the outer segment defects we report appear to be more severe than those observed in the P23H knock-in mouse.^{8,32} Possible explanations for these differences include species-specific differences in the model organism (mouse versus frog), species-specific differences in the P23H rhodopsin gene sequence (mouse versus bovine)⁵ and differences in the type of cell death investigated (cell death in dim light conditions versus cell death exacerbated by bright light). Another possibility is that because cell death in our model is highly synchronized, we may more readily detect ultrastructural changes that are of a transient nature.

In rod inner segments of bP23H-expressing animals exposed to light, we observed compartments with discernable contents in close proximity to the endoplasmic reticulum. The

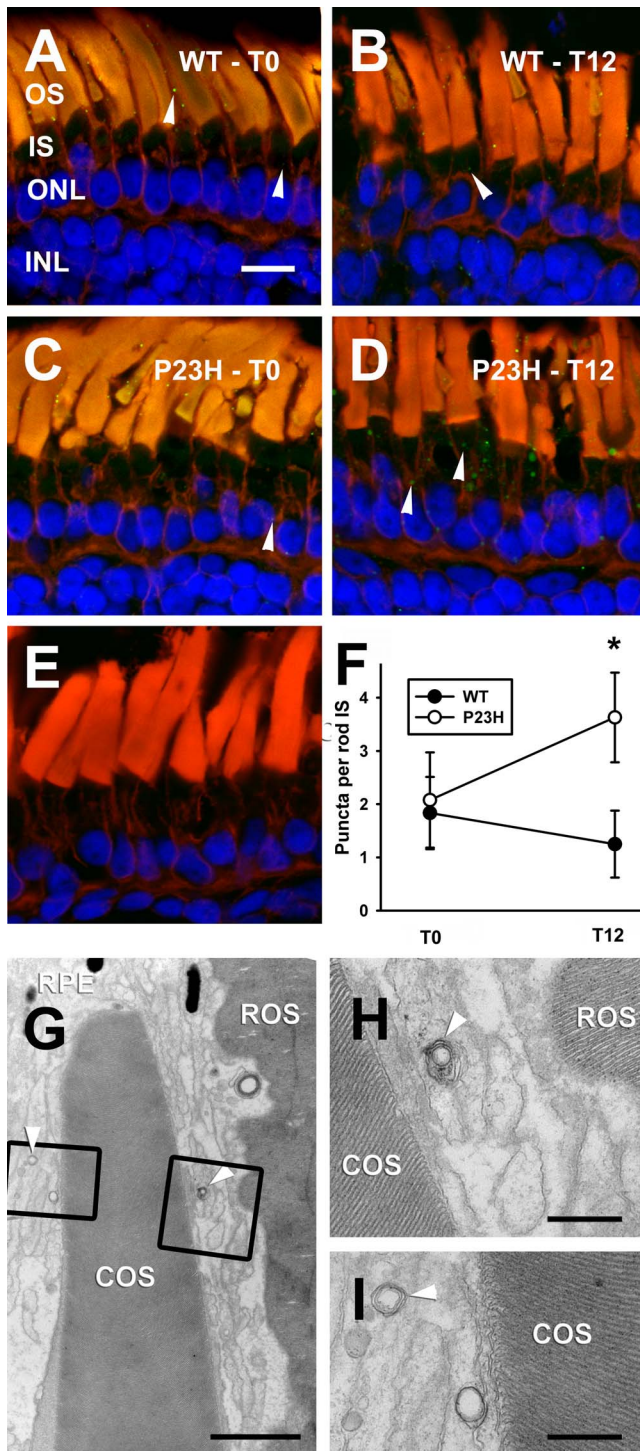


FIGURE 6. LC3B immunolabeling confirmed the presence of increased number of autophagic compartments (*arrowheads*) in rod inner segments of tadpoles expressing bP23H. Images are derived from dark-reared WT tadpole (A); WT tadpole exposed to 12 hours of light (B); dark-reared bP23H-expressing tadpole (C); and bP23H-expressing tadpole exposed to 12 hours of light (D). Puncta are more prominent and more numerous. (E) Wild-type tadpole-control labeling without primary antibody. Quantification of LC3-positive puncta in rod inner segments. *Error bars* = SEM. $n \geq 4$ per group. $*P = 0.041$. (G-I) LC3-positive puncta present in the OS layer are likely associated with interdigitating processes of the RPE. Electron micrographs show no autophagic structures within rod and cone OS (G), but double-membrane compartments are present in interdigitating processes of the RPE (*arrowheads*). (H, I) Further magnification of the boxed regions in (G). *Scale bars*: (A) 10 μm; (G) 2 μm; (H, I) 500 nm.

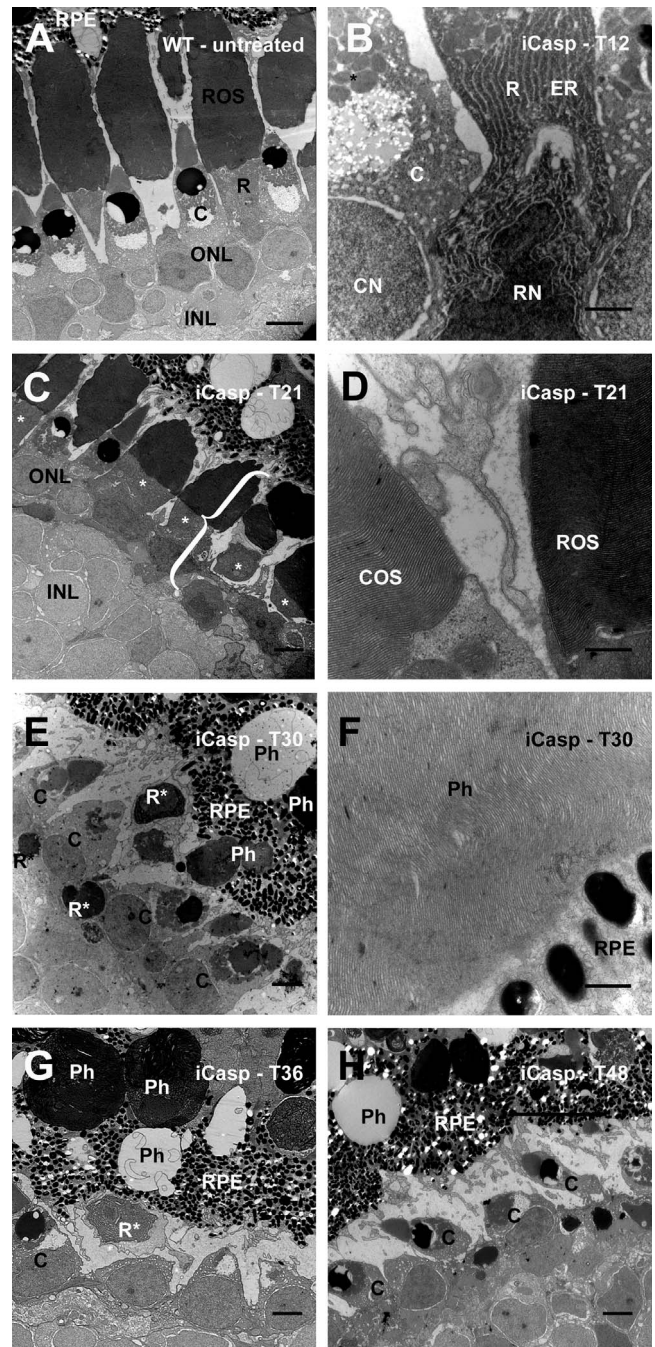


FIGURE 7. Rod outer segment vesiculations and increased number of autophagic compartments were not observed in a drug-induced rod apoptosis model. Images are derived from (A) untreated WT control; and (B) iCasp9-expressing tadpole 12 hours after AP20187 administration. There is minimal evidence of cell death, with darkly staining rod cytoplasm and some evidence of altered nuclear morphology. (C) iCasp9-expressing tadpole 21 hours after AP20187 administration. Rods* stained darkly relative to other cell types, and cell fragmentation was initiated (*bracket*). (D) Rod and cone outer segment (OS) disks retained a high degree of organization at 21 hours. (E) iCasp9-expressing tadpole 30 hours after AP20187. Numerous apoptotic rod remnants are present, and many are undergoing phagocytosis by the RPE. (F) Rod OS remnants in RPE phagosomes retain a high degree of disk organization. (G) iCasp9-expressing retina 36 hours after AP20187 administration. Rod remnants are present in phagosomes of the RPE. (H) iCasp9-expressing retina 48 hours after AP20187 administration (essentially rodless). C, cone; Ph, phagosome; R, rod; R*, apoptotic rod fragment. *Scale bars*: 10 μm (A, C, E-H), 2 μm (B), 500 nm (D, F).

ultrastructure of these compartments was consistent with that of autophagosomes and autolysosomes. Accumulation of LC3B puncta in rod inner segments of light exposed retinas corroborates this hypothesis. Autophagosomes and autolysosomes are hallmarks of autophagy, a process that was first described with the aid of TEM during the 1960s.^{33,34}

The number of autophagic compartments was increased in transgenic *X. laevis* in comparison to wild-type animals kept under similar light conditions, suggesting that autophagy levels in bP23H-expressing rods were above normal.³⁵⁻³⁷ In addition, we did not observe an increase in autophagic compartments in the drug induced rod apoptosis model, in which cell death occurred over a similar time frame. In photoreceptors, the presence of autophagy has been described in developing retinal tissue in mammals³⁸ and also as an adaptation to bright light exposure, accompanied by the subsequent removal of outer segment disks.³⁷ However, in degenerating photoreceptors, autophagy may represent an attempt to eliminate damaged cellular compartments and mutant rhodopsin from the secretory pathway, and therefore may reflect the specific mechanisms of photoreceptor degeneration associated with P23H rhodopsin.

The target substrates of autophagy are likely to be damaged ER, mitochondria, and small protein aggregates, and we observed autophagosome contents consistent with ER membranes in our images. No aggresomes (large aggregates) were observed in the present study, confirming previous results.^{4-6,39} This is likely due to the fact that photoreceptors have low levels of intermediate filament proteins such as vimentin,⁴⁰ which are essential components of the microtubule cytoskeleton required to form aggresomes.^{41,42} It has been hypothesized that protein aggregates are cytotoxic and could cause photoreceptor cell death.^{41,43,44}

Misfolded proteins are known to be ubiquitinated, retrotranslocated from the ER, and degraded by the ubiquitin-proteasome system, but autophagy can also play a role in their removal, and the two processes are closely coupled.⁴⁵ Several misfolded proteins associated with neurodegenerative disorders, including mutant huntingtin and α -synuclein, are degraded by autophagy.⁴⁶⁻⁵⁰ Moreover, saturation of the proteasome can trigger autophagy.⁵¹ It has also been proposed that saturation of the proteasome (proteostatic crisis) may be the trigger for cell death in multiple retinal degenerations,⁵² and the dramatic increase in autophagic compartments we observed on light exposure may be a manifestation of this process.

Although it is not immediately clear from our data whether the retinal degeneration we observed was ultimately due to outer segment or inner segment defects, our previous studies support the involvement of biosynthetic defects in the retinal degeneration process. Notably, similar outer segment membrane defects were observed in the absence of cell death by Haeri et al.⁹ However it is more likely that both processes contribute to cell death to varying degrees. In fact, it is conceivable that certain conditions could favor one mechanism over another; specifically, correction of a biosynthetic defect via the use of pharmacologic chaperones,⁵³ chaperone inducers,⁵⁴ chaperone gene therapy,¹² a more stable form of P23H rhodopsin, according to the present study and that by Tam et al.,⁵⁵ or light deprivation⁵ (as in this study) could increase the delivery of mutant rhodopsin to outer segments, preventing biosynthetic defects but increasing subsequent damage to outer segments on light exposure. We have previously demonstrated a 3-fold increase in bP23H protein levels under dark rearing conditions⁴ such as those used in this study. The identification of autophagic and apoptotic markers in parallel in other studies indicates that photoreceptor degeneration may be influenced by mechanisms besides the

caspase pathways, and that multiple cell death mechanisms may exist.^{16,56}

Autophagy pathways may represent a therapeutic target for rescuing photoreceptors from cell death in RP. Drugs that act as autophagy inducers may be therapeutic candidates for treatment of RP patients with the P23H rhodopsin genotype,³ a subject of ongoing investigations in our laboratory. They would promote the clearing of the mutant rhodopsin from the secretory pathway as well as stimulate the removal of damaged cellular compartments.

In summary, our findings suggest that, in rod photoreceptors expressing P23H rhodopsin, light can trigger both inner and outer segment membrane defects, resulting in retinal degeneration that occurs by type II cell death, also known as cell death with autophagy.¹⁵ The cell death is characterized by the presence of vesiculations in the outer segments, impaired trafficking of outer segment soluble proteins, and an increase in vacuolization, including autophagic vacuolization, near the endoplasmic reticulum. This is consistent with instability of the mutant rhodopsin in both rod outer segments and the secretory pathway upon light exposure.

Acknowledgments

The authors thank David Papermaster for invaluable support. W. Clay Smith generously provided the anti-arrestin antibody. We also acknowledge the technical assistance of Garnet Martens, Derrick Horne, and Bradford Ross, and helpful discussions with Steven Fliesler, Laurie Molday, Susan Shinn, Sharon Gorski, and Wayne Vogl.

Supported by the Canadian Institutes of Health Research Grant MOP-64400, Foundation Fighting Blindness-Canada, National Eye Institute, and professional development grants awarded to TB by the UBC Office of the Vice-President Research and International.

Disclosure: **T.H. Bogéa**, None; **R.H. Wen**, None; **O.L. Moritz**, None

References

1. Sohocki MM, Daiger SP, Bowne SJ, et al. Prevalence of mutations causing retinitis pigmentosa and other inherited retinopathies. *Hum Mutat.* 2001;17:42-51.
2. Dryja TP, McGee TL, Reichel E, et al. A point mutation of the rhodopsin gene in one form of retinitis pigmentosa. *Nature.* 1990;343:364-366.
3. Mendes HF, van der Spuy J, Chapple JP, Cheetham ME. Mechanisms of cell death in rhodopsin retinitis pigmentosa: implications for therapy. *Trends Mol Med.* 2005;11:177-185.
4. Tam BM, Moritz OL. Dark rearing rescues P23H rhodopsin-induced retinal degeneration in a transgenic *Xenopus laevis* model of retinitis pigmentosa: a chromophore-dependent mechanism characterized by production of N-terminally truncated mutant rhodopsin. *J Neurosci.* 2007;27:9043-9053.
5. Tam BM, Qazalbash A, Lee HC, Moritz OL. The dependence of retinal degeneration caused by the rhodopsin P23H mutation on light exposure and vitamin A deprivation. *Invest Ophthalmol Vis Sci.* 2010;51:1327-1334.
6. Lee DC, Vazquez-Chona FR, Ferrell WD, et al. Dysmorphic photoreceptors in a P23H mutant rhodopsin model of retinitis pigmentosa are metabolically active and capable of regenerating to reverse retinal degeneration. *J Neurosci.* 2012;32:2121-2128.
7. Moritz OL, Tam BM. Recent insights into the mechanisms underlying light-dependent retinal degeneration from *X. laevis* models of retinitis pigmentosa. *Adv Exp Med Biol.* 2010;664:509-515.

8. Sakami S, Maeda T, Bereta G, et al. Probing mechanisms of photoreceptor degeneration in a new mouse model of the common form of autosomal dominant retinitis pigmentosa due to P23H opsin mutations. *J Biol Chem*. 2011;286:10551-10567.
9. Haeri M, Knox BE. Rhodopsin mutant P23H destabilizes rod photoreceptor disk membranes. *PLoS One*. 2012;7:e30101.
10. Lin JH, Li H, Yasumura D, et al. IRE1 signaling affects cell fate during the unfolded protein response. *Science*. 2007;318:944-949.
11. Lin JH, Lavail MM. Misfolded proteins and retinal dystrophies. *Adv Exp Med Biol*. 2010;664:115-121.
12. Gorbatyuk MS, Knox T, LaVail MM, et al. Restoration of visual function in P23H rhodopsin transgenic rats by gene delivery of BiP/Grp78. *Proc Natl Acad Sci U S A*. 2010;107:5961-5966.
13. Organisciak DT, Vaughan DK. Retinal light damage: mechanisms and protection. *Prog Retin Eye Res*. 2010;29:113-134.
14. Levine B, Kroemer G. Autophagy in the pathogenesis of disease. *Cell*. 2008;132:27-42.
15. Kroemer G, Levine B. Autophagic cell death: the story of a misnomer. *Nat Rev Mol Cell Biol*. 2008;9:1004-1010.
16. Lohr HR, Kuntchithapautham K, Sharma AK, Rohrer B. Multiple, parallel cellular suicide mechanisms participate in photoreceptor cell death. *Exp Eye Res*. 2006;83:380-389.
17. Kunchithapautham K, Rohrer B. Autophagy is one of the multiple mechanisms active in photoreceptor degeneration. *Autophagy*. 2013;3:65-66.
18. Kunchithapautham K, Rohrer B. Apoptosis and autophagy in photoreceptors exposed to oxidative stress. *Autophagy*. 2012;3:433-441.
19. Kunchithapautham K, Coughlin B, Lemasters JJ, Rohrer B. Differential effects of rapamycin on rods and cones during light-induced stress in albino mice. *Invest Ophthalmol Vis Sci*. 2011;52:2967-2975.
20. Hamm LM, Tam BM, Moritz OL. Controlled rod cell ablation in transgenic *Xenopus laevis*. *Invest Ophthalmol Vis Sci*. 2009;50:885-892.
21. Lee DC, Hamm LM, Moritz OL. *Xenopus laevis* tadpoles can regenerate neural retina lost after physical excision but cannot regenerate photoreceptors lost through targeted ablation. *Invest Ophthalmol Vis Sci*. 2013;54:1859-1867.
22. Tam BM, Moritz OL. The role of rhodopsin glycosylation in protein folding, trafficking, and light-sensitive retinal degeneration. *J Neurosci*. 2009;29:15145-15154.
23. Adamus G, Zam ZS, Arendt A, Palczewski K, McDowell JH, Hargrave PA. Anti-rhodopsin monoclonal antibodies of defined specificity: characterization and application. *Vis Res*. 1991;31:17-31.
24. MacKenzie D, Arendt A, Hargrave P, McDowell JH, Molday RS. Localization of binding sites for carboxyl terminal specific anti-rhodopsin monoclonal antibodies using synthetic peptides. *Biochemistry*. 1984;23:6544-6549.
25. Venable JH, Coggeshall R. A simplified lead citrate stain for use in electron microscopy. *J Cell Biol*. 1965;25:407-408.
26. Peterson JJ, Tam BM, Moritz OL, et al. Arrestin migrates in photoreceptors in response to light: a study of arrestin localization using an arrestin-GFP fusion protein in transgenic frogs. *Exp Eye Res*. 2003;76:553-563.
27. Moritz OL, Tam BM, Papermaster DS, Nakayama T. A functional rhodopsin-green fluorescent protein fusion protein localizes correctly in transgenic *Xenopus laevis* retinal rods and is expressed in a time-dependent pattern. *J Biol Chem*. 2001;276:28242-28251.
28. Eskelinen E-L. To be or not to be? Examples of incorrect identification of autophagic compartments in conventional transmission electron microscopy of mammalian cells. *Autophagy*. 2008;4:257-260.
29. Calvert PD, Strissel KJ, Schiesser WE, Pugh EN, Arshavsky VY. Light-driven translocation of signaling proteins in vertebrate photoreceptors. *Trends Cell Biol*. 2006;16:560-568.
30. Mann SS, Hammarback JA. Molecular characterization of light chain 3. A microtubule binding subunit of MAP1A and MAP1B. *J Biol Chem*. 1994;269:11492-11497.
31. Rubinsztein DC, Cuervo AM, Ravikumar B, et al. In search of an "autophagometer." *Autophagy*. 2009;5:585-589.
32. Chiang W-C, Kroeger H, Sakami S, et al. Robust endoplasmic reticulum-associated degradation of rhodopsin precedes retinal degeneration. *Mol Neurobiol*. 2015;52:679-695.
33. Ashford TP, Porter KR. Cytoplasmic components in hepatic cell lysosomes. *J Cell Biol*. 1962;12:198-202.
34. Deter RL, De Duve C. Influence of glucagon, an inducer of cellular autophagy, on some physical properties of rat liver lysosomes. *J Cell Biol*. 1967;33:437-449.
35. Remé CE, Knop M. Autophagy in frog visual cells in vitro. *Invest Ophthalmol Vis Sci*. 1980;19:439-456.
36. Remé C, Drinker CK, Aeberhard B. Modification of autophagic degradation by medium- and illumination conditions in frog visual cells in vitro. *Doc Ophthalmol*. 1984;56:377-383.
37. Remé CE, Wolfrum U, Imsand C, Hafezi F, Williams TP. Photoreceptor autophagy: effects of light history on number and opsin content of degradative vacuoles. *Invest Ophthalmol Vis Sci*. 1999;40:2398-2404.
38. Guimarães CA, Benchimol M, Amarante-Mendes GP, Linden R. Alternative programs of cell death in developing retinal tissue. *J Biol Chem*. 2003;278:41938-41946.
39. Tam BM, Moritz OL. Characterization of rhodopsin P23H-induced retinal degeneration in a *Xenopus laevis* model of retinitis pigmentosa. *Invest Ophthalmol Vis Sci*. 2006;47:3234-3241.
40. Nakazawa T, Takeda M, Lewis GP, et al. Attenuated glial reactions and photoreceptor degeneration after retinal detachment in mice deficient in glial fibrillary acidic protein and vimentin. *Invest Ophthalmol Vis Sci*. 2007;48:2760-2768.
41. Kopito RR. Aggresomes, inclusion bodies and protein aggregation. *Trends Cell Biol*. 2000;10:524-530.
42. Illing ME, Rajan RS, Bence NF, Kopito RR. A rhodopsin mutant linked to autosomal dominant retinitis pigmentosa is prone to aggregate and interacts with the ubiquitin proteasome system. *J Biol Chem*. 2002;278:28.
43. Chiang W-C, Messah C, Lin JH. IRE1 directs proteasomal and lysosomal degradation of misfolded rhodopsin. *Mol Biol Cell*. 2012;23:758-770.
44. Chiang W-C, Hiramoto N, Messah C, Kroeger H, Lin JH. Selective activation of ATF6 and PERK endoplasmic reticulum stress signaling pathways prevent mutant rhodopsin accumulation. *Invest Ophthalmol Vis Sci*. 2012;53:7159-7166.
45. Yao T-P. The role of ubiquitin in autophagy-dependent protein aggregate processing. *Genes Cancer*. 2010;1:779-786.
46. Ravikumar B, Duden R, Rubinsztein DC. Aggregate-prone proteins with polyglutamine and polyalanine expansions are degraded by autophagy. *Hum Mol Genet*. 2002;11:1107-1117.
47. Webb JL, Ravikumar B, Atkins J, Skepper JN, Rubinsztein DC. Alpha-Synuclein is degraded by both autophagy and the proteasome. *J Biol Chem*. 2003;278:25009-25013.
48. Corrochano S, Renna M, Tomas-Zapico C, et al. α -Synuclein levels affect autophagosome numbers in vivo and modulate Huntington disease pathology. *Autophagy*. 2012;8:431-432.
49. Winslow AR, Chen CW, Corrochano S, et al. Alpha-synuclein impairs macroautophagy: implications for Parkinson's disease. *J Cell Biol*. 2010;190:1023-1037.
50. Sarkar S, Ravikumar B, Rubinsztein DC. Autophagic clearance of aggregate-prone proteins associated with neurodegeneration. *Methods Enzymol*. 2009;453:83-110.

51. Kruse KB, Brodsky JL, McCracken AA. Autophagy: an ER protein quality control process. *Autophagy*. 2015;2:135-137.
52. Lobanova ES, Finkelstein S, Skiba NP, Arshavsky VY. Proteasome overload is a common stress factor in multiple forms of inherited retinal degeneration. *Proc Natl Acad Sci U S A*. 2013; 110:9986-9991.
53. Noorwez SM, Kuksa V, Imanishi Y, et al. Pharmacological chaperone-mediated in vivo folding and stabilization of the P23H-opsin mutant associated with autosomal dominant retinitis pigmentosa. *J Biol Chem*. 2003;278:14442-14450.
54. Kosmaoglou M, Schwarz N, Bett JS, Cheetham ME. Molecular chaperones and photoreceptor function. *Prog Retin Eye Res*. 2008;27:434-449.
55. Tam BM, Noorwez SM, Kaushal S, Kono M, Moritz OL. Photoactivation-induced instability of rhodopsin mutants T4K and T17M in rod outer segments underlies retinal degeneration in *X. laevis* transgenic models of retinitis pigmentosa. *J Neurosci*. 2014;34:13336-13348.
56. Arango-Gonzalez B, Trifunović D, Sahaboglu A, et al. Identification of a common non-apoptotic cell death mechanism in hereditary retinal degeneration. *PLoS One*. 2014;9:e112142.